

# Integrated treatment of refinery wastewater using oxidized cotton waste ( $\text{H}_2\text{O}_2/\text{NaOH}/\text{CW}$ ) as adsorbent and photodegradation

## ABSTRACT

A new environmentally acceptable method for manufacturing high carboxyl content (CC) oxidized cotton waste (OCW) utilizing  $\text{H}_2\text{O}_2/\text{NaOH}$  has been developed to enhance the surface and pore size of prepared material by removing hemicellulose, lignin, and impurities and then treated chemically to produce free radicals from oxidized waste cotton by hydrogen peroxide. The structure and morphology of the resulting OCW were meticulously considered using various techniques, including titration, EDX, XRD, FTIR, TGA, and FE-SEM. It was observed that the degree of polymerization, yield, and crystallinity of OCW was influenced by the NaOH concentration and exhibited variations in different directions. FTIR analysis indicated successful selective oxidation of the hydroxide groups of CW. XRD and FE-SEM results revealed thorough oxidation penetration throughout the waste cotton, disrupting its consistency and length while preserving its crystal structure. This paper presents a straightforward green approach for fabricating OCW with high crystallinity and specific surface area. The resulting OCW holds promise for applications such as adsorption and photodegradation of organic pollutants in refinery wastewater (RWW), contributing to environmental sustainability.

**Keywords:** water treatment, adsorption, cotton, composite and oxidation processes.

## Introduction

Water is essential for sustaining all life forms and plays a pivotal role in maintaining the integrity and sustainability of Earth's ecosystems [1]. However, in recent years, the availability and accessibility of fresh water have emerged as critical issues. Water contamination has become a significant threat to humanity, with domestic households contributing to the discharge of oily wastewater that pollutes seas, rivers, groundwater, and lakes [2]. This contamination arises from various sources such as oil refineries, dyes, paper mills, textile dyes, detergents, surfactants, pesticides, herbicides, insecticides, and pharmaceutical manufacturers [3]. The proliferation of contaminated water poses a serious challenge as it renders water unfit for daily consumption and usage [4]. Addressing this issue is imperative to protect both human well-being and the environment

[5]. Therefore, wastewater should be treated before being discharged into the soil or the aquatic systems by using practical treatment methods [6].

Many previous studies have investigated the ability of the use of different types of treatment processes to eliminate pollutants from wastewater and to overcome the crisis of continuous freshwater demands worldwide according to stringent environmental regulations [7]. The wastewater treatment encompasses physical, chemical, and biological techniques such as sorption [8], coagulation [9], precipitation [10], ion exchange [11], electrochemical treatment [12], membrane filtration, and biodegradation [13]. However, traditional biological and chemical methods often need to catch up due to the non-biodegradable nature of many pollutants. Moreover, conventional wastewater treatment processes are costly or ineffective, merely transferring pollutants between phases rather than eliminating them [14]. Despite membrane filtration's ability to produce high-quality water, its susceptibility to fouling adds to operational expenses [15].

To address these challenges, the adsorption process emerges as an efficient and economical means of removing organic, pigments, and other colorants from wastewater. Activated carbons are commonly utilized due to their high adsorption capacity and microporous structure [16]. However, commercial activated carbon is cost-prohibitive, prompting the search for alternative low-cost adsorbents [17]. Cotton, comprising over 90% cellulose, is a promising candidate due to its widespread availability, affordability, renewability, durability, and biodegradability. Surface chemical modifications of cellulosic nanomaterials have been explored by incorporating various inorganic and organic functional groups to enhance adsorption capabilities [18,19]. Combining adsorption with chemical processes can effectively remove organics from solutions and achieve higher maximum adsorption capacities [20]. Hydrogen peroxide is a green and inexpensive oxidant for fabricating oxidized cellulose, offering advantages over oxidizing agents like periodate and permanganate [21]. This study focuses on fabricating CW with high carboxyl content using a two-step method involving the preparation of  $H_2O_2/NaOH/CW$ . It evaluates its efficacy for organic removal in refinery wastewater through physical and chemical processes. Optimization of parameters such as cotton waste type, reaction time, pH, temperature, and UV light exposure will be conducted to determine the optimal conditions for batch technical applications.

## **Experimental**

### **Chemical and Instrumentation Test**

The sample of refinery wastewater with organic pollutants discharged from an oilfield refinery plant in Iraq was stored in a polypropylene container at 4°C for treatment by adsorption and oxidation

technologies as listed in Table 1. The chemical compounds utilized in this investigation were of the analytical grade. H<sub>2</sub>SO<sub>4</sub> and NaCl were purchased from Scharlau, Spain. Hydrogen peroxide (German, 45 % wt), as well as NaOH (99 % purity) and carbon tetra chloride from India, are the organic pollutants in wastewater according to the lecture [22].

Equation (1) was used for organic removal :

$$Y_{OCRE} = \frac{A_o - A_t}{A_o} \times 100\% \quad (1)$$

Anywhere:  $Y_{OCRE}$  is organic elimination;  $A_o$ ,  $A_t$  organic concentration before and after the treatment (mg organic/L) respectively.

**Table 1** Refinery wastewater specification

No.	Limit	Concentration(mg/L)	No.	Limit	Concentration(mg/L)
1	Oil content	165.3 (mg/L)	6	Conductivity	510000 $\mu$ s/cm
2	COD	265 ppm	7	TDS	326400 (mg/L)
3	Turbidity	24.79 NTU	8	Viscosity	1.0103 m Pa/S
4	Dissolved oxygen content	0.032 (mg/L)	9	TSS	15.2 (mg/L)
5	Specific gravity	0.9965	10		

### Preparation of H<sub>2</sub>O<sub>2</sub>/NaOH/CW

The waste cotton was washed with hot water to clean from wastes and added to NaOH solution to prepare NaOH/CW according to the author[23] with some modifications. The CW with NaOH was then desiccated at 75 °C in an oven aimed at 24 hrs to produce NaOH/CW. Next, the alkali-treated cotton waste was added to a solution containing 2% acetic acid and 7% hydrogen peroxide as presented in Fig.1 .The alkali CW was added to 2 % acetic acid and 9 % hydrogen peroxide under UV light for 19 hours [24] with some requirements.

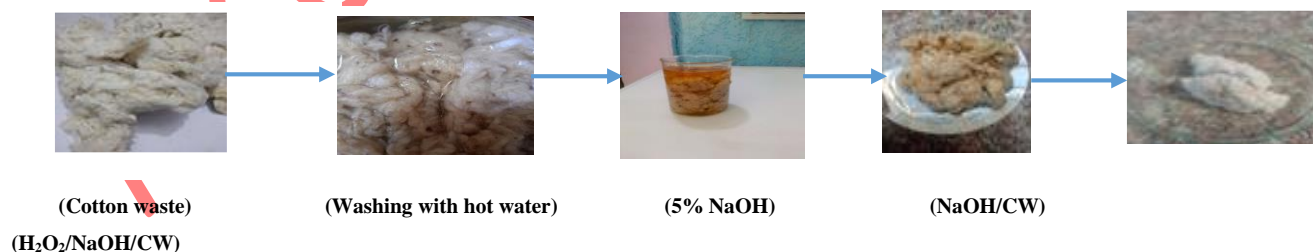


**Fig. 1.** Preparation of H<sub>2</sub>O<sub>2</sub>/NaOH/CW

### Residual of hydrogen peroxide

The residual amount of H<sub>2</sub>O<sub>2</sub> is quantified using a method involving a slightly acidified potassium iodide (K<sub>I</sub>) solution in the attendance of the amount of ammonium molybdate by way of a

catalyst. In this process, the hydrogen peroxide oxidizes the potassium iodide, liberating iodine in the solution. The unconventional iodine is titrated with a thiosulfate solution, with starch acting as an indicator [25].

### Carboxyl content determination

The carboxyl content in oxidized cotton waste was strong-minded using a titration technique described by Saida et al. [26]. 50 mL of a 2% calcium acetate contained 0.4 gm of the H<sub>2</sub>O<sub>2</sub>/NaOH/CW and titrated with 0.1 N, a NaOH solution.

$$\text{Carboxyl group} = \frac{Nx(Vc-Vb)xM_{\text{COOH}}}{\text{OWC}(mg)} \times 100\% \quad (2)$$

### Batch adsorbent and photodegradation experiments

The adsorption/photodegradation experimentations were used in a 250 mL batch oxidation reactor with a UV light source. The intensity of UV light was maintained at 0.5 mW/cm<sup>2</sup>. A stirring velocity of approximately 200 rpm agitated the RWW at different times ranging from 30 to 120 minutes. Before adding reagents, the pH of the solutions was adjusted using dilute solutions of sodium hydroxide or sulfuric acid. Various amounts of oxidized cotton waste (ranging from 0.5 to 1.5 grams) were utilized in the experiments as shown in Fig.2.



Fig.2. Adsorption and photodegradation treatment.

## Experimental design

This work demonstrated the optimization of untried conditions for the mineralization and pollutants of refinery wastewater using the adsorption and photodegradation treatment. Design Expert Minitab-17 program with Box-Bingham design is used for graphical depiction, arithmetical analysis, and quadratic model removal with time (30-120 min), pH (3-9), Dose (0.5-1.5 gm), temperature (25-70), and UV light (2-8).

## Results and Discussion

### Effects that affect oxidized groups

A complete study was conducted into the influence of numerous limits on the growth of carboxyl groups in CW. The untried circumstances for the various examples were as trails: Fig. 3a presented the slow effect of H<sub>2</sub>O<sub>2</sub>; Fig. 3b showed the temperature effect with agent concentration; Figure 3c presented the effect of pH; and Figure 3d found the effect of time. The consequences of the study showed that the production of carboxyl content in prepared materials was likewise wedged by various working circumstances. The quantity of OCW was powerfully influenced by the H<sub>2</sub>O<sub>2</sub>. Increasing the agent concentration leads to an increase in the carboxyl groups reaching a highest of 9% as shown in Fig. 3a. However, H<sub>2</sub>O<sub>2</sub> must be additional in restraint to produce carboxyl content on cotton waste. [27, 28]. The pH of the solution influenced the oxidation reaction by affecting the release rate of reactive hydroxyl radicals. Higher initial pH values led to higher carboxylate content, indicating a more considerable oxidation result under base conditions [29]. With increasing pH, the carboxyl groups rose slowly until they peaked at pH 9.0. Smaller times led to imperfect oxidations and reduced functional groups [30].

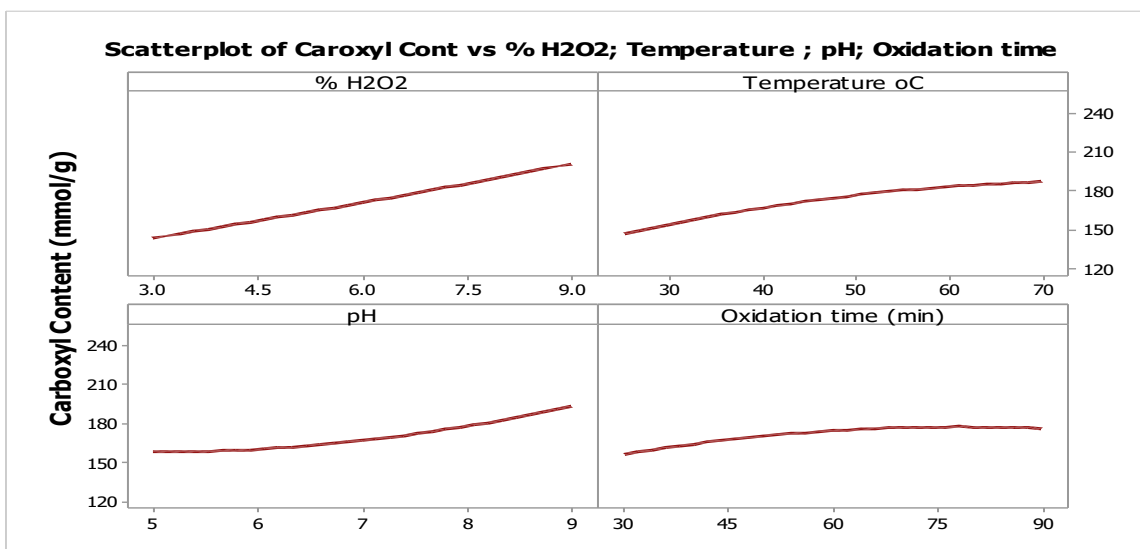


**Fig.3.** Parameters that affect the carboxyl content on (a) hydrogen peroxide, (b) temperature (c) pH, and (d) oxidation time

### The mechanism of Oxidation

Fig. 4 proposes and exemplifies the CW oxidation technique. The vicissitudes in cotton structures over time are presented in Fig. 4a. The crystal structure first vicissitudes from cellulose I to cellulose II next infiltration by alkaline solution. This increased accessibility facilitates the number of hydroxyl groups by H<sub>2</sub>O<sub>2</sub> within the solid-liquid reaction system [30]. The oxidation mechanism of H<sub>2</sub>O<sub>2</sub> is illustrated in Fig. 4b. Under UV light, H<sub>2</sub>O<sub>2</sub> decomposes to generate free radicals. This hydroxyl radical bouts the carbon atom at the C-6 position, facilitated by the inductive effect of the adjacent hydroxyl group [31].

The hydroxyl group oxidizes to aldehyde groups as a consequence of the unbalanced structure that consequences, which is shared with carbon. The augmented OH concentration then saves the aldehyde groups oxidized to carboxyl groups. The ionization of carboxyl content throughout this oxidation procedure causes the pH of the solution to droplet. Also, the amorphous portion of CW is hydrolyzed, thus, upsurges in crystallinity consequence in reductions in yield. Deprived of altering the crystal structure of H<sub>2</sub>O<sub>2</sub>/NaOH/CW [32].

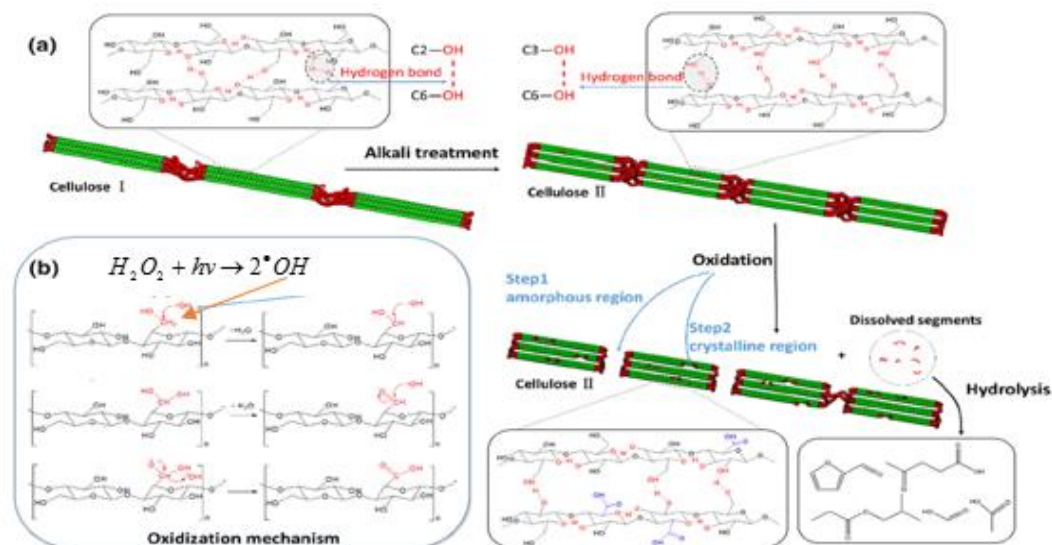


Fig. 4. Structure alteration of the cellulose (a) and the oxidation mechanism (b)

### The characteristics of $H_2O_2/NaOH/CW$

The oxidation reaction induces structural alterations in cotton waste macromolecules. To investigate the changes in treated CW's chemical composition, FT-IR spectroscopy was used. The spectra for CW, NaOH/CW, and  $H_2O_2/NaOH/CW$  are shown in Fig. 5, respectively. Following treatment, there was a noticeable decrease in relative intensities at  $3600\text{--}3000\text{ cm}^{-1}$ , which corresponds to  $\text{--OH}$  stretching vibrations mainly from the presence of hydroxyl groups in cotton waste. This reduction demonstrated a noteworthy decline in the number of hydroxyl groups following treatment, indicating a partial disruption of hydrogen bond structures in waste cotton and, as a result, a reduction in waste cotton's mechanical capabilities, was noted with increasing degrees of oxidation and oxidized group content. This shift is attributed to the formation or incorporation of aldehyde and carboxylate groups during the oxidation degumming. Additionally, the FT-IR spectrum of treated cotton waste revealed distinctive absorption peaks, including O–H stretching at around  $3420\text{ cm}^{-1}$ ,  $\text{CH}_2$  symmetric bending at approximately  $1420\text{ cm}^{-1}$ , and C–O–C stretching at about  $1060\text{ cm}^{-1}$ . These intensities displayed subtle alterations due to the oxidative impact of hydrogen peroxide [33].

Fig. 6 shows the XRD spectra of oxidized cotton waste with varying CC. Sharp peaks are observed at  $2\theta = 22.59$ , indicating the typical pattern of type I cellulose for CW. The crystallinity of the samples exhibits diverse variations. The crystallinity of cotton waste reductions after

pretreatment with alkali was initially attributed to the destruction of hydrogen bonds in the cellulose I crystals during the alkali treatment process [34].

This reduction in crystallinity occurs because the regular arrangement of cellulose molecular chains is disrupted. However, the crystallinity significantly increases upon oxidation, nearly reaching 100.0% for OCW. This increase in crystallinity is attributed to several factors. The destruction of hydrogen bonds during alkali pretreatment increases the accessibility of waste cotton, making hydroxyl groups more susceptible to oxidation by hydrogen peroxide; primary hydroxyl groups in the amorphous region are preferentially oxidized to carboxyl groups during the oxidation process, and oxidation results in the formation of water-soluble fragments and a decline in the molecular weight of cellulose. Consequently, the region of amorphous cotton waste is mainly removed, leaving only the crystalline region behind. As a result, the crystallinity of oxidized cotton waste increases to 100.0% and stabilizes with the increase in carboxylate content. This indicates a transformation from amorphous to crystalline structure, driven by oxidation and the consequent elimination of amorphous regions. In high content, (OCW High) images, more intense defibrillation is observed with less unaffected fibers than with alkali-treated waste cotton. Notably, only a tiny portion of the total cotton waste fraction was approved through a 1-micron membrane filter, and the amount was nearly the same for cotton waste and OCW. The fractionation work indicated that only a tiny portion of the processed cotton fell within the size range of OCW. Figs.6(a- f) depicts the structural differences between CW and OCW [35].

In Fig.7b, alkali pretreatment induces crystal transformation, reducing crystallinity and resulting in volume variations for cotton waste and compared with CW in Fig.7c,e, and f as presented in the lecture [36]. The images show cotton waste entangled to form bundle-like structures with smooth surfaces and straight shapes. Conversely, in Fig.7c, the surfaces of OCW with different carboxylate contents appear coarser than that of waste cotton, with a few cracks visible on the cotton surface. Also, the roughness of the cotton surface increases with higher CC [37]. This phenomenon is likely caused by etching from the oxidant, as observed in the images. Fig.7 also illustrates that hydrogen peroxide can penetrate the entire waste cotton, ensuring the oxidation reaction occurs within the cotton. Consequently, the partial dissolution of OCW in water generates cavities within the cotton structure [38].

This observation indicates the effectiveness of  $H_2O_2$  in facilitating the oxidation process throughout the cotton waste. The energy dispersive X-ray (EDX) analysis checked the purity of the

prepared composite samples. The samples consisted of C and O elements, as seen in Fig.8a. Furthermore, no impurity peaks are visible, indicating that the sample is pure [39].

Fig. 8b demonstrates the TGA of the CW. TGA was secondhand to inspect the examples' weight loss and thermal constancy as the temperature increased to 200 °C, a 5.75% initial weight damage was well-known, which was credited to the vanishing of volatile materials comprised in the moisture and CW. After the prepared sample was heated from 285 to 380 °C, there was a significant 78% weight loss. General, when likened to before published investigation, the prepared oxidized cotton waste showed moderately alike thermal characteristics [40].

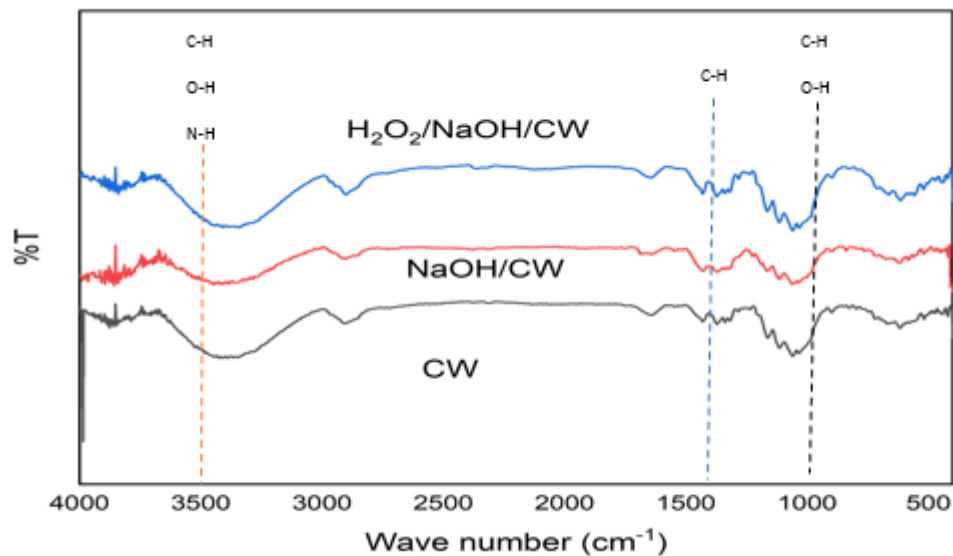
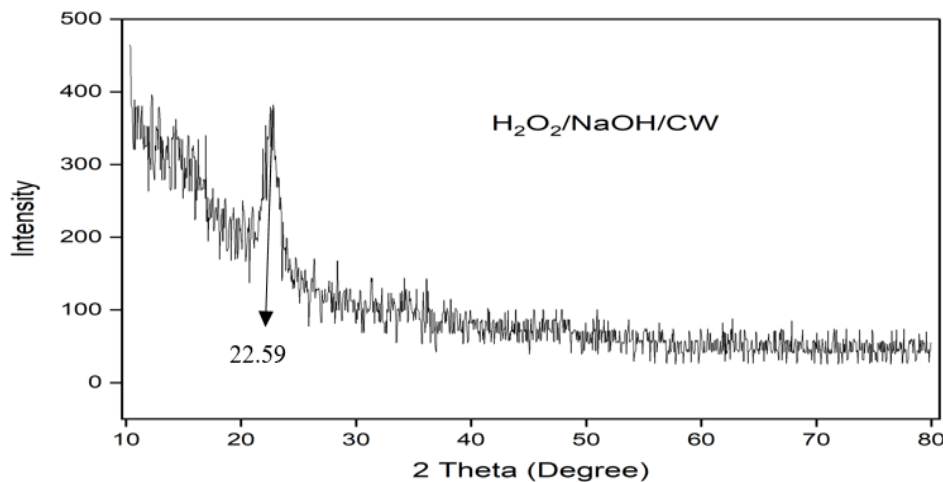
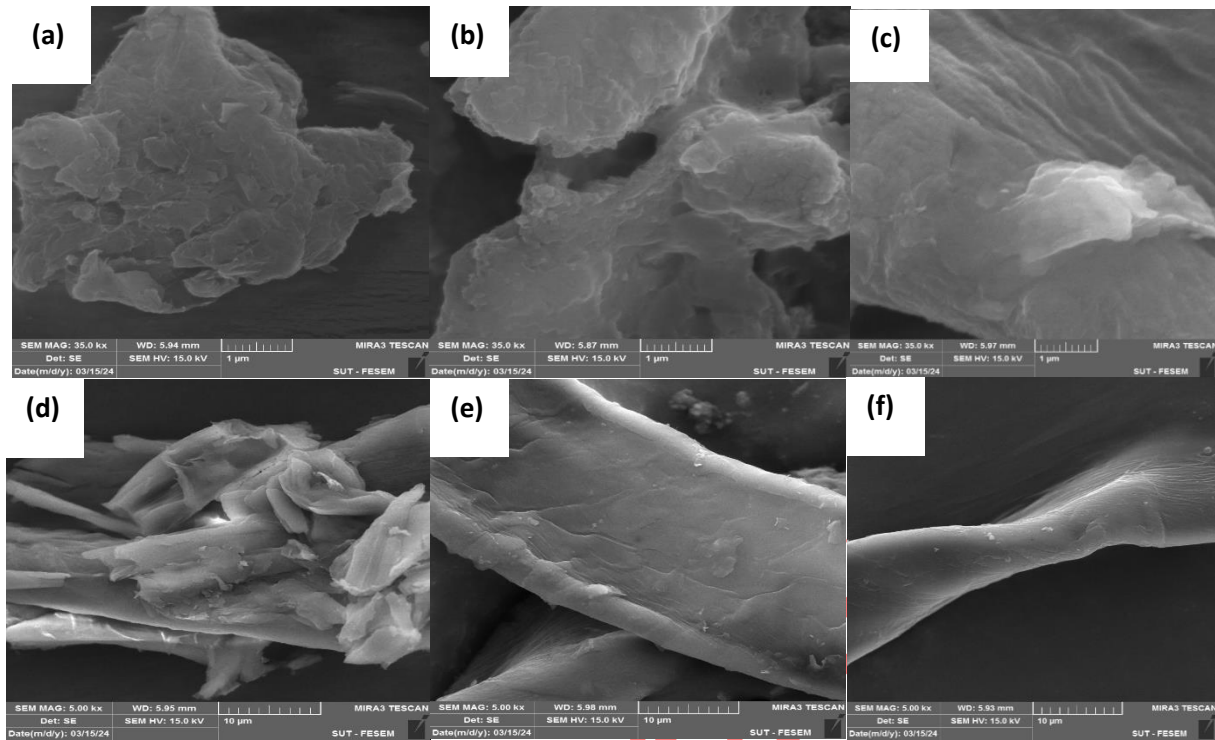


Fig.5. FTIR of CW and composites



**Fig. 6.** XRD analysis for H<sub>2</sub>O<sub>2</sub>/NaOH/CW



**Fig. 7.** FE SEM photographs of (a) cotton waste at 10 μm, (b) Alkali CW at 10 μm, (c) OCW at 10 μm, (d) cotton waste at 1 μm, (e) and (f) OCW at 1 μm

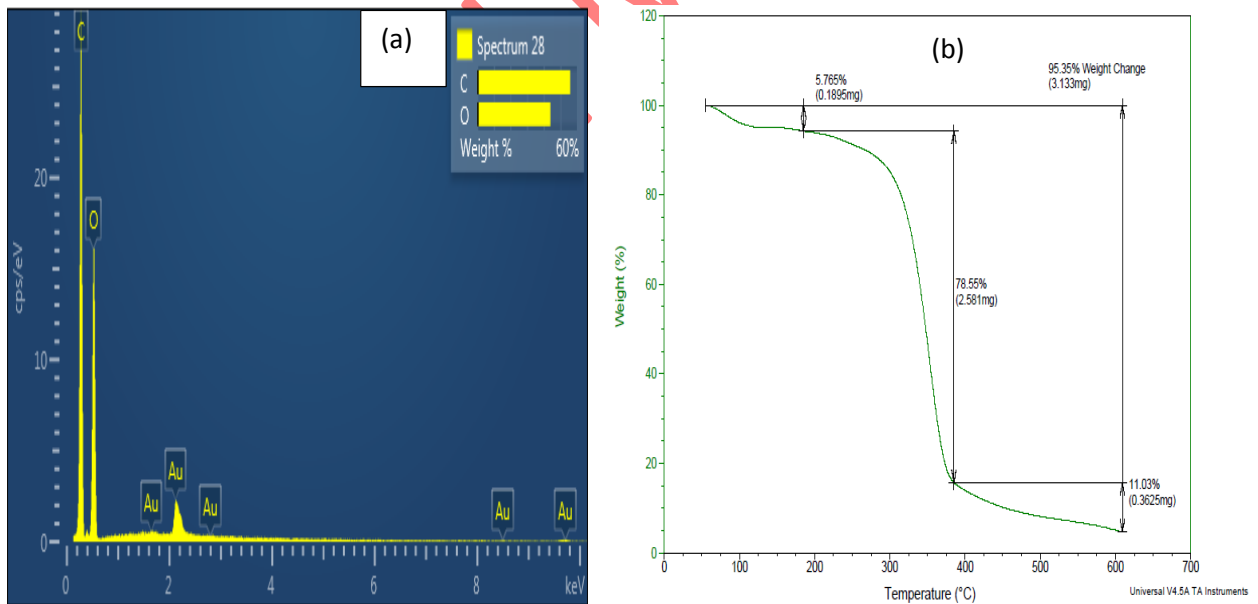


**Fig. 8.** H<sub>2</sub>O<sub>2</sub>/NaOH/CW analysis of (a) EDX and (b) TGA

## Modeling of adsorption/photodegradation

The recovery of organic by way of function oxidation time, pH, dose, temperature, and UV lamps of cotton waste oxidation are shown in equations (3-5) for CW, NaOH/CW, and H<sub>2</sub>O<sub>2</sub>/NaOH/CW respectively.

$$Y_{CW}=8.9+ 0.109 X_1+ 4.96 X_2+ 5.2 X_3- 0.026 X_4- 2.22 X_5- 0.000334 X_1^2- 0.326 X_2^2- 1.21 X_3^2+ 0.00023 X_4^2+ 0.108 X_5^2- 0.0019 X_1X_2- 0.0267 X_1X_3 + 0.00115 X_1X_4+ 0.0007 X_1X_5+ 0.35 X_2X_3- 0.0170 X_2X_4+ 0.269 X_2X_5+ 0.084 X_3X_4+ 0.38 X_3X_5 + 0.0281 X_4X_5 \quad (3)$$

$$Y_{NaOH/CW}=14.1+ 0.063 X_1+ 5.13 X_2+ 41.5 X_3+ 0.370 X_4+0.14 X_5- 0.352 X_2^2- 9.51 X_3^2- 0.00182 X_4^2+ 0.041 X_5^2+0.0057 X_1X_2- 0.029 X_1X_3+ 0.001 06 X_1X_4- 0.0009 X_1X_5+ 0.22 X_2X_3- 0.0229 X_2X_4+ 0.275 X_2X_5- 0.147 X_3X_4 - 1.23 X_3X_5 + 0.0332 X_4X_5 \quad (4)$$

$$Y_{H2O2/NaOH/CW}=12.8+ 0.020 X_1+ 4.17 X_2+ 38.6 X_3+ 0.356 X_4- 0.47 X_5+ 0.000031 X_1^2- 0.342 X_2^2- 8.58 X_3^2- 0.00183 X_4^2+ 0.116 X_5^2+ 0.0080 X_1X_2- 0. 022 X_1X_3+ 0.00118 X_1X_4- 0.0043 X_1X_5+ 0.53 X_2X_3- 0.0198 X_2X_4+ 0.329 X_2X_5- 0.148 X_3X_4- 1.35 X_3X_5 + 0.0329 X_4X_5 \quad (5)$$

Where X<sub>1</sub> is the oxidation time, X<sub>2</sub> is the pH, X<sub>3</sub> is the dose, X<sub>4</sub> is the temperature and X<sub>5</sub> is the UV Lamps.

As shown in Fig. 9, the main belongings plots demonstrate the perfect set of vital limits for attaining the obligatory oxidation presentation for OCW. The best set of parameters for a given adsorption and photodegradation presentation is shown in each plot [19].

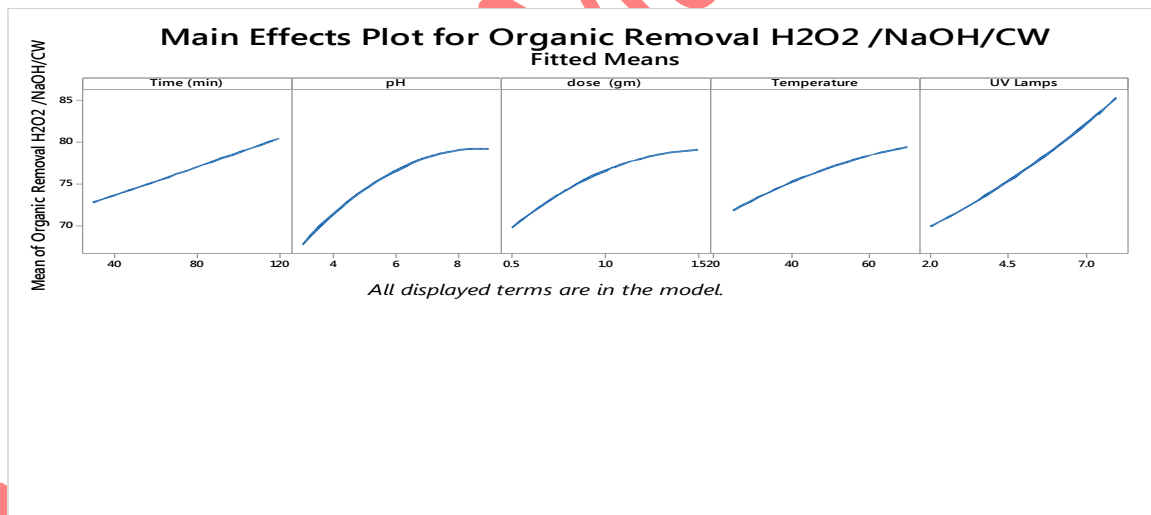


Fig. 9. Main effects plot for organic removal.

The consequences exposed in Fig. 10, for all oil pollutants with values for OCW, the efficiency of the removal response recovers with time throughout the reaction. In these circumstances, the reaction material's incomplete surface area inclines to cause a drop at an exact spot, making it more difficult to get a moderately high elimination ratio [41].

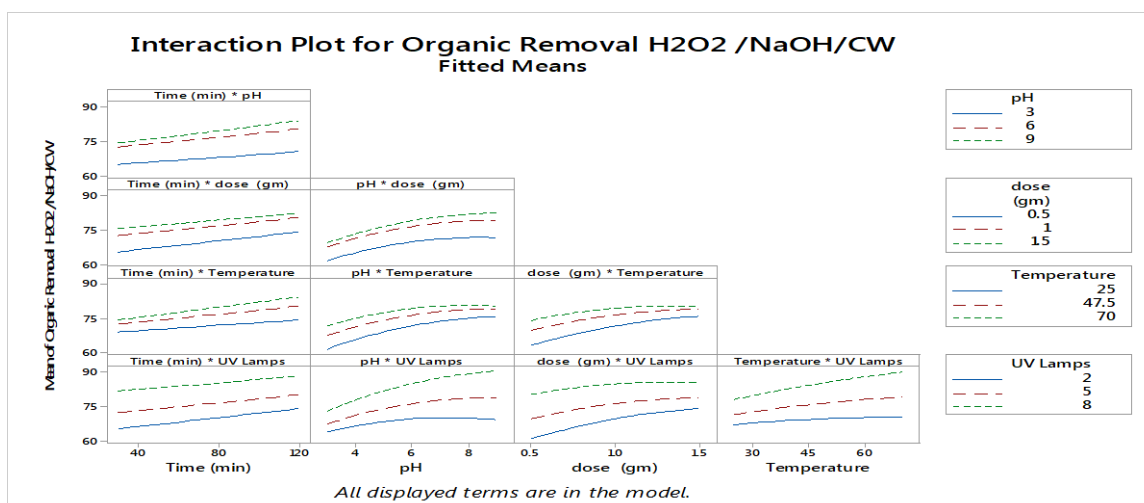


Fig. 10. Interaction plot of parameters

### The adsorption and photodegradation

To determine how the oxidation time variable affected the adsorption and oxidation treatment and how effective it was at getting rid of organic pollutants in RWW, a purposeful analysis of the variable was carried out. For this work, other variables were kept constant. Based on photo-oxidation principles, the formation of free radicals with high oxidizing capacity occurs during the process. These free radicals oxidize the organic pollutants, leading to the breakdown of ions within a short time [42]. Fig.11a illustrates the relationship between organic removal efficiency and time (adsorption and oxidation) throughout the combined process. Experiments were carried out to find the best time for adsorption and oxidation efficiency in eliminating organic from wastewater. With the increase in time, the elimination efficiency is enhanced [43].

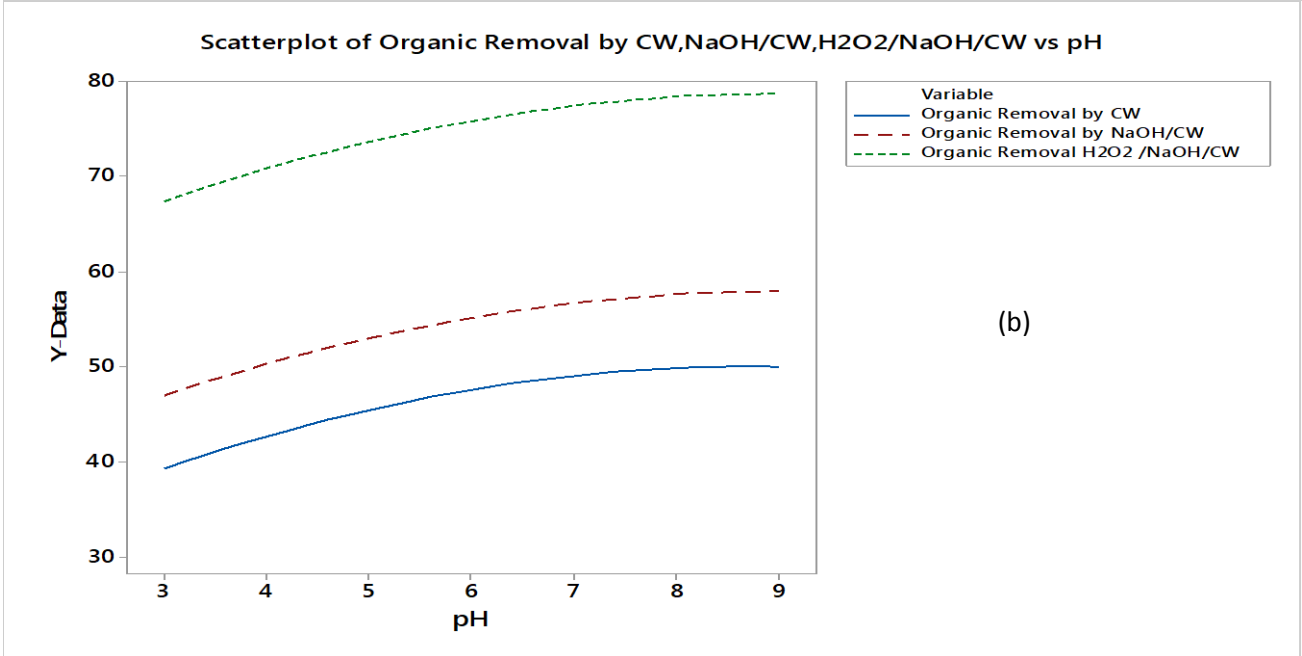
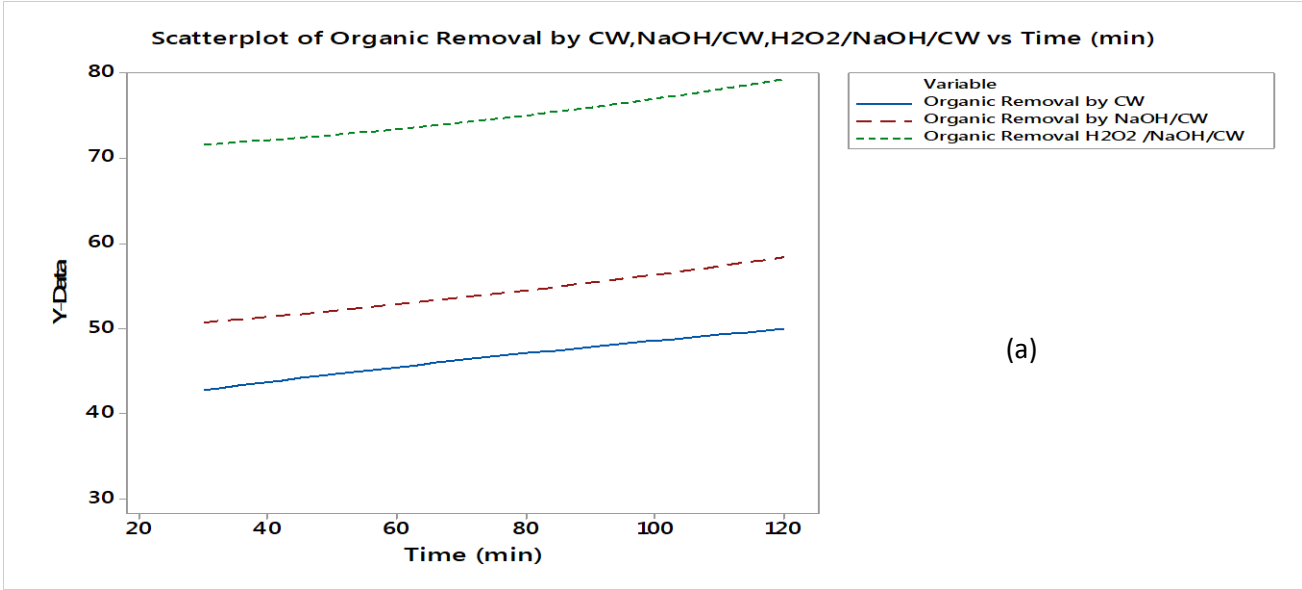
An upsurge in organic removal has been related to free radicals oxidizing pollutants material. The consequences were in line with another study that presented that spreading the oxidation period recovers process competence, as exposed by [44]. The pH in adsorption and oxidation systems is an important influence on the uptake of organic pollutants due to its control over the surface charge of solid particles, the kinds of potentially determining current ions, in addition to the extent of the adsorbed species' ionization and speciation [45]. Utilizing a pH range of 3 to 9 and a contact time of 120 min, all trials were led to inspect the influence of pH on the adsorption of organic pollutants by CW using H<sub>2</sub>O<sub>2</sub> and NaOH. The highest adsorption and oxidation competencies for 46.9.3, 57.9, and 77.8% at pH 9 for CW, NaOH/CW, and OCW were corresponding, as shown in Fig.11b [46].

Fig. 11c demonstrates that the quantity of organic oxidation upsurges rapidly by way of the dose of CW increases [47], the removal efficiency has increased as the total amount of adsorbent and that is enhanced adsorption and oxidation treatment (47.1, 56.8, and 76.3 % For CW, NaOH/CW,

and H<sub>2</sub>O<sub>2</sub>/NaOH/CW respectively). A higher amount of adsorbent increases the probability of solid particle collision and, thus, particle aggregation. As the number of particles increases, the adsorption effectiveness improves. This is because of the increased surface area for adsorption [48].

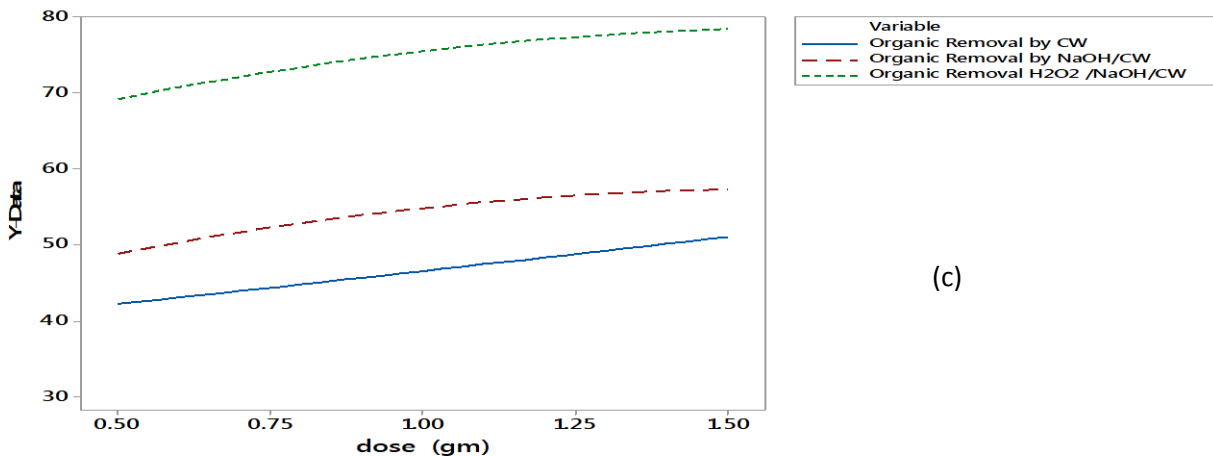
The temperature of the reaction is another crucial limit that significantly influences the degradation process. This study employed different temperatures ranging from 25 to 70°C while keeping the amounts of reagents. Fig.11d illustrates the removal efficiency of organic pollutants for experiments conducted at various temperatures, the influence of temperature on the removal efficiency can be observed as a positive effect on wastewater treatment. The removal rises significantly as the temperature increases from 25 to 70°C. For instance, at 25°C, the removal efficiency is 41.2%, 51.5%, and 71% for CW, NaOH/CW, and H<sub>2</sub>O<sub>2</sub>/NaOH/CW, respectively. However, at 70°C, the removal efficiency increases to 48.5%, 58.6%, and 78% for the same treatments, representing the enhanced efficiency at higher temperatures. This positive correlation between temperature and removal efficiency can be attributed to the faster reaction rates at high temperatures [49]. The increase in temperature promotes the oxidation process, leading to higher levels of oxidized group content, However, it is crucial to maintain the temperature within certain appropriate limits to prevent excessive damage to the cotton structure and to achieve optimal cotton waste efficiency [50].

The last limiting factor controlling the rate of the oxidation process is the intensity of light exposure. To investigate the impact of UV light on the effectiveness of cotton waste oxidation to remove organic pollutants from wastewater, each with an intensity of 0.5 mW/cm<sup>2</sup> and a wavelength of 365 nm [51]. Different configurations of UV lamps (2, 4, and 8) were tested in the batch oxidation process to assess their influence on the organic elimination efficiency of waste cotton, NaOH, and H<sub>2</sub>O<sub>2</sub>-treated cotton waste while keeping all other parameters and quantities constant. Fig.11e presents the results of the number of lamps on the organic efficiency targeting wastewater. The results indicate that the efficiency was enhanced with an increasing number of cumulative UV-A lamps, ranging from one to three. This observation is consistent with previous findings [47].



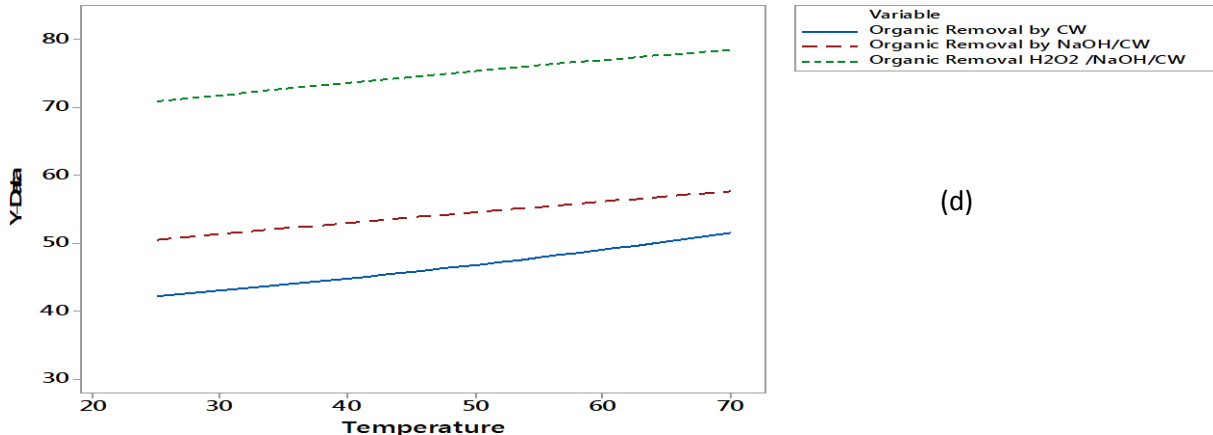
ACCEPTED

Scatterplot of Organic Removal by CW,NaOH/CW ,H2O2/NaOH/CW vs dose (gm)



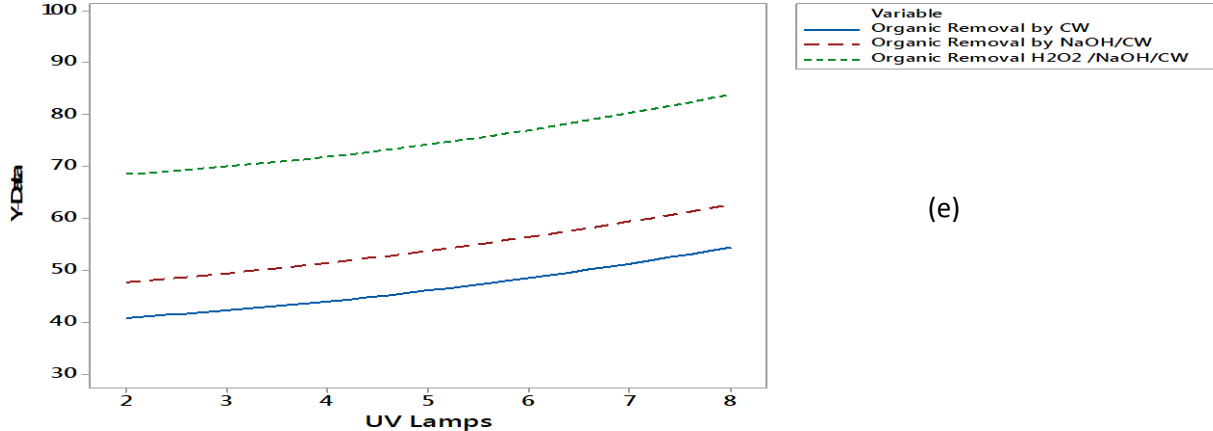
(c)

Scatterplot of Organic Removal by CW,NaOH/CW,H2O2/NaOH/CW vs Temperature



(d)

Scatterplot of Organic Removal by CW, NaOH/CW,H2O2/NaOH/CW vs UV Lamps



(e)

Fig.11. Effect of the working parameters on organic removal (a) time, (b) pH, (c) dose, (d) temperature, and (e) UV light.

Optimization of operational parameters

The best working limits, counting prepared oxide dose, pH, irradiation time, temperature, and UV lamps, are found under ideal investigational circumstances aimed at the cotton wastes and prepared oxide material Fig. 12 shows the best organic removal with Minitab software. When associated with similar studies in Table 3, the present work with another and compared between them.

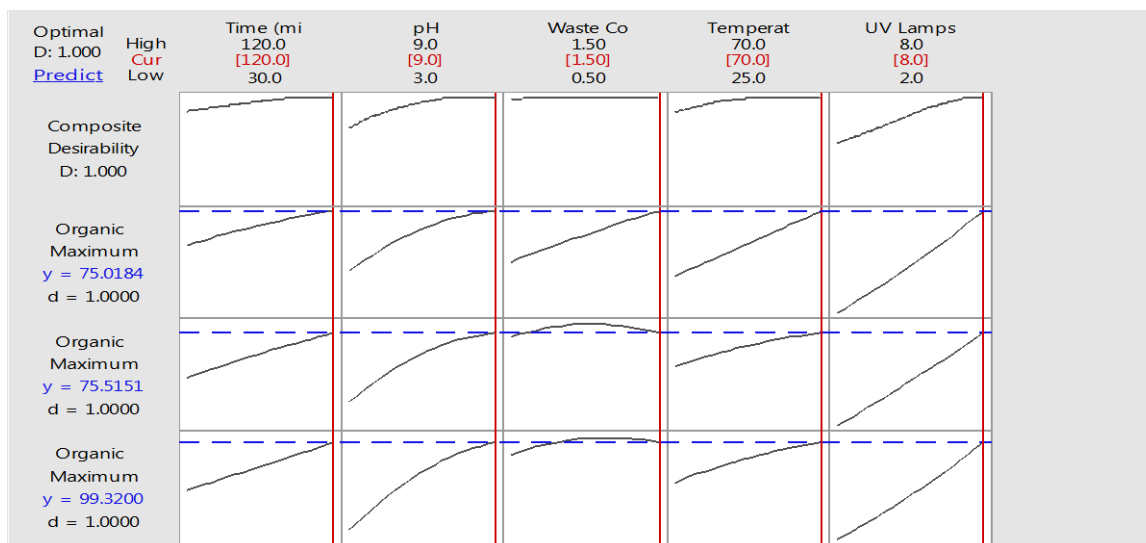


Fig. 12. Finest employed variables on refinery wastewater

Table 3. Comparison of the current study with other described studies

Photocatalyst	Organic Pollutants	Irradiation Type	Time (min)	Degradation Efficiency	Ref.
ZnO, TiO <sub>2</sub> and Al <sub>2</sub> O <sub>3</sub>	Organic pollutants	Solar	120	95.2 % and 92.11%, 80.7% for ZnO,TiO <sub>2</sub> and Al <sub>2</sub> O <sub>3</sub>	[52]
TiO <sub>2</sub> / bentonite	hydrocarbons	UV	120	93%	[53]
ZnO/Cellulose Acetate	dyes	UV	20	75%	[54]
H <sub>2</sub> O <sub>2</sub> /NaOH/CW	Organic pollutants	UV	120	96.3%	This work

### Kinetic model for oxidation

The effect of H<sub>2</sub>O<sub>2</sub> addition on the photodegradation of organic pollutants over NaOH/CW. The adsorbent was investigated under specific conditions: 1 gm dose, 50 min reaction time, and pH = 7. The results established that as agent concentrations increased, more free radicals were made, which assisted in the reaction of organic pollutants and accelerated the oxidation. Nonetheless, there was an impartial slight upsurge in organic oxidation, going from 94.5% to 96.3% when the hydrogen peroxide amount was increased from 7% to 9%. Considering cost-effectiveness, the H<sub>2</sub>O<sub>2</sub> of 7% was deemed suitable for further study [55]. The first-order model is expressed

$$\ln\left[\frac{C_o}{C}\right] = K_1 t \quad (6)$$

$C_o, C_t$  = initial concentration of organic mg/l (before and after treatment)

$t$  = time in minutes.

$K_1$  = the first order rate constant ( $\text{min}^{-1}$ ).

The best correlation between oxidation time and the left side of the Equation was found in the kinetics investigation for OCW, as exposed in Fig.13. This proposes a pseudo-first-order kinetic model. When the agent concentration was kept at 7%, the prepared oxide showed a first-order degradation coefficient ( $k_1$ ) value of  $0.077 \text{ min}^{-1}$ .

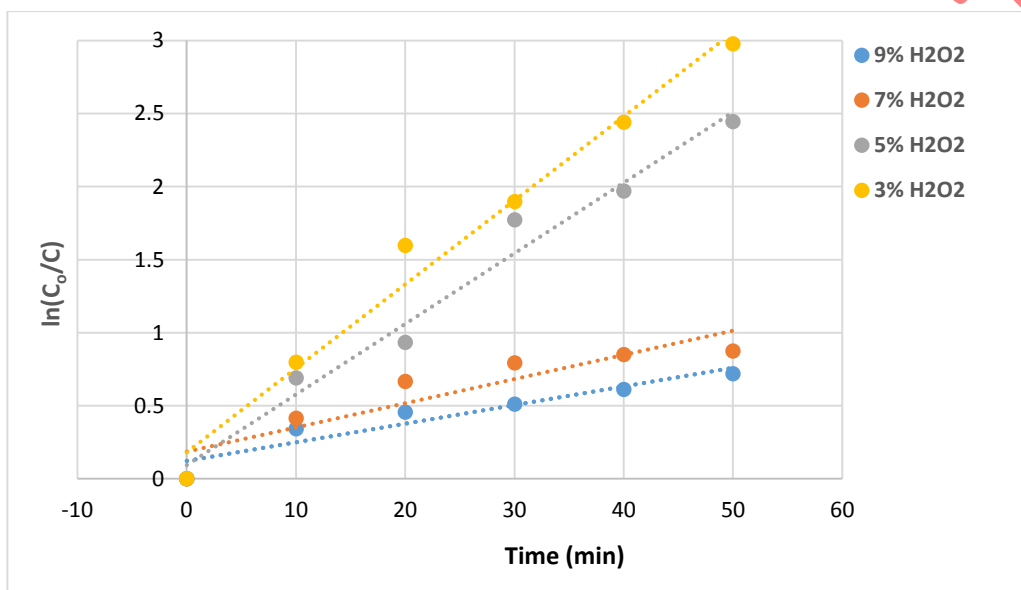


**Fig.13.** Plot of  $-\ln(C/C_o)$  vs. time for the organic photodegradation

## Conclusion

The oxidation competence is notably enhanced by pretreating cotton waste with NaOH solution, which increases its accessibility to the oxidizing agents. Optimized reaction conditions were determined to achieve high CC in OCW through a green and convenient method involving NaOH pretreatment followed by  $\text{H}_2\text{O}_2/\text{UV}$  oxidation. This approach can also change usual carbohydrates into furfural and other soluble organic compounds using the  $\text{H}_2\text{O}_2$  oxidant system. The study demonstrates high removal efficiencies when employing  $\text{H}_2\text{O}_2/\text{NaOH}/\text{CW}$  for organic removal in RWW across all dosages. Even at lower dosages,  $\text{H}_2\text{O}_2/\text{NaOH}/\text{CW}$  exhibits superior removal efficiencies compared to NaOH/CW and CW alone, with efficiencies increasing to 96.3%, 73.1%, and 64.8%, respectively, at higher dosages. Furthermore, the oxidation pretreatment results in an OCW product containing a higher proportion of small, well-fibrillated particles, as evidenced through fractionation and scanning electron microscopy analysis, compared to alkali and other

pretreatment methods studied. This indicates the effectiveness of the proposed method in producing OCW with desirable characteristics for various applications.

### Acknowledgment

We extend our sincerest appreciation to the Chemical Engineering Department, Engineering College, Baghdad University, for their invaluable support and resources that made this research possible.

### Reference

- [1] H. A. Ibrahim, A. A. Hassan, A. H. Ali, and H. M. Kareem, "Organic removal from refinery wastewater by using electro catalytic oxidation," in *AIP Conference Proceedings*, AIP Publishing, 2023, <https://doi.org/10.1063/5.0163257>.
- [2] A. S. Atiyah, A. A. A. Al-Samawi, and A. A. Hassan, "Photovoltaic cell electro-Fenton oxidation for treatment oily wastewater," *AIP Conf. Proc.*, vol. 2235, no. May, 2020, <https://doi.org/10.1063/5.0008937>.
- [3] M. K. Ibrahim, A. A. Al-Hassan, and A. S. Naje, "Utilisation of cassia surattensis seeds as natural adsorbent for oil content removal in oilfield produced water," *Pertanika J. Sci. Technol.*, vol. 27, no. 4, pp. 2123–2138, 2019, <https://doi.org/10.13140/RG.2.2.18444.28807>.
- [4] A. A. Hassan, R. T. Hadi, A. H. Rashid, and A. S. Naje, "Chemical modification of castor oil as adsorbent material for oil content removal from oilfield produced water," *Pollut. Res.*, vol. 39, no. 4, pp. 892–900, 2021, [http://www.envirobiotechjournals.com/article\\_abstract.php?aid=11057&iid=323&jid=4](http://www.envirobiotechjournals.com/article_abstract.php?aid=11057&iid=323&jid=4).
- [5] W. Zhang *et al.*, "Nanoscale bioconjugates: A review of the structural attributes of drug-loaded nanocarrier conjugates for selective cancer therapy," *Heliyon*, vol. 8, no. 6, p. e09577, 2022, <https://doi.org/10.1016/j.heliyon.2022.e09577>.
- [6] G. F. Naser, I. H. Dakhil, and A. A. Hasan, "Organic pollutants removal from oilfield produced water using nano magnetite as adsorbent," *Glob. NEST J.*, vol. 23, no. 3, pp. 381–387, 2021, <https://doi.org/10.30955/gnj.003875>.
- [7] F. Y. AlJaberi, "Desalination of groundwater by electrocoagulation using a novel design of electrodes," *Chem. Eng. Process. - Process Intensif.*, vol. 174, no. June 2021, p. 108864, 2022, <https://doi.org/10.1016/j.cep.2022.108864>.
- [8] R. Del Sole, A. A. Fogel, V. A. Somin, G. Vasapollo, and L. Mergola, "Evaluation of Effective Composite Biosorbents Based on Wood Sawdust and Natural Clay for Heavy Metals Removal from Water," *Materials (Basel)*, vol. 16, no. 15, 2023, <https://doi.org/10.3390/ma16155322>.
- [9] S. Deswal, S. Rawat, S. Kumar, and V. Sangwan, "Potential of Moringa oleifera and Okra as Coagulants in Sustainable Treatment of Water and Wastewater," *Ecol. Quest.*, vol. 34, no. 4, pp. 1–17, 2023, <https://doi.org/10.12775/eq.2023.045>.
- [10] F. Y. AlJaberi, D. R. Hadi, and S. K. Ajjam, "Electrocoagulation Treatment of Textile Wastewater: A Review," *AIP Conf. Proc.*, vol. 2806, no. 1, 2023, <https://doi.org/10.1063/5.0163278>.
- [11] A. Q. Saeed, B. Y. Al-Zaidi, A. S. Hamadi, H. S. Majdi, and A. A. AbdulRazak, "Upgrade of heavy crude oil via aquathermolysis over several types of catalysts," *Mater. Express*, vol. 12, no. 2, pp. 278–287, 2022, <https://doi.org/10.1166/mex.2022.2139>.
- [12] R. D. Nsaif, S. F. Alturki, M. S. Suwaed, and A. A. Hassan, "Lead removal from refinery wastewater by using photovoltaic electro Fenton oxidation," in *AIP Conference Proceedings*, AIP Publishing, 2023, <https://doi.org/10.1063/5.0163378>.

- [13] H. R. D. Alamery, A. A. Hassan, and A. H. Rashid, "Copper Removal in Simulated Wastewater by Solar Fenton Oxidation," *AIP Conf. Proc.*, vol. 2806, no. 1, 2023, <https://doi.org/10.1063/5.0167259>.
- [14] K. M. Mousa Al-Zobai and A. A. Hassan, "Utilization of Iron Oxide Nanoparticles (Hematite) as Adsorbent for Removal of Organic Pollutants in Refinery Wastewater," in *Materials Science Forum*, Trans Tech Publ, 2022, pp. 91–100. <https://www.scientific.net/MSF.1065.91>.
- [15] R. Abdullah *et al.*, "Fabrication of composite membrane with microcrystalline cellulose from lignocellulosic biomass as filler on cellulose acetate based membrane for water containing methylene blue treatment," *Bioresour. Technol. Reports*, vol. 25, no. November 2023, p. 101728, 2024, <https://doi.org/10.1016/j.biteb.2023.101728>.
- [16] A. N. Hammadi and I. K. Shakir, "Adsorption Behavior of Light Naphtha Components on Zeolite (5A) and Activated Carbon," *Iraqi J. Chem. Pet. Eng.*, vol. 20, no. 4, pp. 27–33, 2019, <https://doi.org/10.31699/ijcpe.2019.4.5>.
- [17] A. A. Jock, M. Ibrahim, S. K. Nuhu, and A. J. Anietie, "Preparation of Activated Carbon Adsorbent From Coconut Husk for the Adsorption of Lead (Ii) Ions From Aqueous Solution," *Niger. J. Trop. Eng.*, vol. 16, no. 1, pp. 1–10, 2022, <https://doi.org/10.59081/njte.16.1.001>.
- [18] S. Rizal *et al.*, "Cotton wastes functionalized biomaterials from micro to nano: A cleaner approach for a sustainable environmental application," *Polymers (Basel)*, vol. 13, no. 7, pp. 1–36, 2021, <https://doi.org/10.3390/polym13071006>.
- [19] H. T. Naem, A. A. Hassan, and R. T. Al-Khateeb, "Wastewater-(Direct red dye) treatment-using solar fenton process," *J. Pharm. Sci. Res.*, vol. 10, no. 9, pp. 2309–2313, 2018, [https://www.researchgate.net/publication/328234109\\_Wastewater-Direct\\_red\\_dye\\_treatment-using\\_solar\\_fenton\\_process](https://www.researchgate.net/publication/328234109_Wastewater-Direct_red_dye_treatment-using_solar_fenton_process).
- [20] K. C. Jun, A. Buthiyappan, and A. A. Abdul Raman, "Application of magnetic-biomass-derived activated carbon as an adsorbent for the treatment of recalcitrant wastewater," *Chem. Pap.*, vol. 75, no. 10, pp. 5279–5295, 2021, <https://doi.org/10.1007/s11696-021-01679-8>.
- [21] G. Ö. Kayan and A. Kayan, "Composite of Natural Polymers and Their Adsorbent Properties on the Dyes and Heavy Metal Ions," *J. Polym. Environ.*, vol. 29, no. 11, pp. 3477–3496, 2021, <https://doi.org/10.1007/s10924-021-02154-x>.
- [22] H. K. Sultan, H. Y. Aziz, B. H. Maula, A. A. Hasan, and W. A. Hatem, "Evaluation of Contaminated Water Treatment on the Durability of Steel Piles," *Advances in Civil Engineering*, vol. 2020, p. 1269563, 2020., <https://doi.org/10.1155/2020/1269563>.
- [23] T. Theivasanthi, F. L. A. Christma, A. Joshua, and S. C. B. Gopinath, "International Journal of Biological Macromolecules Synthesis and characterization of cotton fiber-based nanocellulose," *Int. J. Biol. Macromol.*, vol. 109, pp. 832–836, 2018, <https://doi.org/10.1016/j.ijbiomac.2017.11.054>.
- [24] N. Zang and X. Qian, "Influence of organic acid on thermal hazard of hydrogen peroxide," *Procedia Eng.*, vol. 45, pp. 526–532, 2012, <https://doi.org/10.1016/j.proeng.2012.08.198>.
- [25] A. Heijnesson-hulte and P. Hellstro, "The effect of Fenton chemistry on the properties of microfibrillated cellulose," *Cellul. Springer Verlag*, 2014, <https://doi.org/10.1007/s10570-014-0243-1>.
- [26] S. Benghanem, A. Chetouani, M. Elkolli, and M. Bounekhel, "ScienceDirect Grafting of oxidized carboxymethyl cellulose with hydrogen peroxide in presence of Cu ( II ) to chitosan and biological elucidation," *Integr. Med. Res.*, no. Ii, pp. 1–9, 2017, <https://doi.org/10.1016/j.bbe.2016.09.003>.
- [27] X. Xu, N. Lu, S. Wang, M. Huang, S. Qu, and F. Xuan, "Extraction and Characterization of Microfibrillated Cellulose from Discarded Cotton Fibers through Catalyst Preloaded Fenton Oxidation," *Adv. Mater. Sci. Eng.*, vol. 2021, 2021, <https://doi.org/10.1155/2021/5545409>.

- [28] S. Zaccaron, U. Henniges, A. Potthast, and T. Rosenau, "How alkaline solvents in viscosity measurements affect data for oxidatively damaged celluloses . Cuoxam and Cadoxen," *Carbohydr. Polym.*, vol. 240, no. April, p. 116251, 2020, <https://doi.org/10.1016/j.carbpol.2020.116251>.
- [29] T. Ngulube, "Removal of cationic and anionic dyes from aqueous solution using a clay-based nanocomposite," *Journal of Environmental Chemical Engineering*, vol. 8, no. 2, p. 180, 2019, <https://doi.org/10.1016/j.jece.2019.103582>.
- [30] Z. Li, C. Meng, and C. Yu, "Analysis of oxidized cellulose introduced into ramie fiber by oxidation degumming," *Text. Res. J.*, p. 11, 2015, <https://doi.org/10.1177/0040517515581589>.
- [31] E. Vismara *et al.*, "Nanocellulose from cotton waste and its glycidyl methacrylate grafting and allylation: Synthesis, characterization and adsorption properties," *Nanomaterials*, vol. 11, no. 2, pp. 1–26, 2021, <https://doi.org/10.3390/nano11020476>.
- [32] J. Wen, Y. Yin, X. Peng, and S. Zhang, "Using H<sub>2</sub>O<sub>2</sub> to selectively oxidize recyclable cellulose yarn with high carboxyl content," *Cellulose*, vol. 1, 2019, <https://doi.org/10.1007/s10570-018-2217-1>.
- [33] S. M. Al-Jubouri, "The static aging effect on the seedless synthesis of different ranges FAU-type zeolite Y at various factors," *Iraqi J. Chem. Pet. Eng.*, vol. 20, no. 4, pp. 7–13, 2019, <https://doi.org/10.31699/ijcpe.2019.4.2>.
- [34] Z. Xu *et al.*, "Synthesis of char-based adsorbents from cotton textile waste assisted by iron salts at low pyrolysis temperature for Cr(VI) removal," *Environ. Sci. Pollut. Res.*, vol. 27, no. 10, pp. 11012–11025, 2020, <https://doi.org/10.1007/s11356-019-07588-4>.
- [35] S. M. Al-Jubouri, H. A. Sabbar, H. A. Lafta, and B. I. Waisi, "Effect of synthesis parameters on the formation 4a zeolite crystals: Characterization analysis and heavy metals uptake performance study for water treatment," *Desalin. Water Treat.*, vol. 165, pp. 290–300, 2019, <https://doi.org/10.5004/dwt.2019.24566>.
- [36] U. A. Qureshi, B. H. Hameed, and M. J. Ahmed, "Adsorption of endocrine disrupting compounds and other emerging contaminants using lignocellulosic biomass-derived porous carbons: A review," *J. Water Process Eng.*, vol. 38, no. September, p. 101380, 2020, <https://doi.org/10.1016/j.jwpe.2020.101380>.
- [37] H. Wilson, "Investigation into non-aqueous remedial conservation treatments for iron-tannate dyed organic materials," p. 512, 2012, <https://www.escholar.manchester.ac.uk/uk-ac-man-scw:191168>
- [38] B. P. De Oliveira, L. T. Moriyama, and V. S. Bagnato, "Colorimetric analysis of cotton textile bleaching through H<sub>2</sub>O<sub>2</sub> activated by UV light," *J. Braz. Chem. Soc.*, vol. 29, no. 6, pp. 1360–1365, 2018, <https://doi.org/10.21577/0103-5053.20170235>.
- [39] T. H. Mhawesh and Z. T. Abd Ali, "Reuse of Brick Waste as a Cheap-Sorbent for the Removal of Nickel Ions from Aqueous Solutions," *Iraqi J. Chem. Pet. Eng.*, vol. 21, no. 2, pp. 15–23, 2020, <https://doi.org/10.31699/ijcpe.2020.2.3>.
- [40] S. H. Mohamed *et al.*, "Recycling waste cotton cloths for the isolation of cellulose nanocrystals: A sustainable approach," *Polymers (Basel)*, vol. 13, no. 4, pp. 1–17, 2021, <https://doi.org/10.3390/polym13040626>.
- [41] A. S. Fahem and A. H. Abbar, "Treatment of petroleum refinery wastewater by electro-Fenton process using porous graphite electrodes," *Egyptian Journal of Chemistry*, vol. 63, no. 12, pp. 4805–4819, 2020, <https://doi.org/10.21608/EJCHEM.2020.28148.2592>.
- [42] A. S. Jafer, R. Al-Khateeb, B. Alobaid, A. Atiyah, and A. A. Hassan, "Copper removal from produced water by photo Fenton oxidation," in *AIP Conference Proceedings*, AIP Publishing, 2023, <https://doi.org/10.1063/5.0165033>.
- [43] A. A. Hassan, F. Y. AlJaberi, and R. T. AL-Khateeb, "Batch and Continuous Photo-Fenton

- Oxidation of Reactive-Red Dye from Wastewater,” *J. Ecol. Eng.*, vol. 23, no. 1, pp. 14–23, 2022, <https://doi.org/10.12911/22998993/143864>.
- [44] F. Y. AlJaberi, “Treatment of Refinery Wastewater by Chemical Advanced Oxidation Processes (UV-photolysis, Fenton, and photo-Fenton): A Comparative Study,” *Iran. J. Chem. Chem. Eng.*, vol. 42, no. 8, pp. 2708–2718, 2023, [https://ijcce.ac.ir/article\\_701405.html](https://ijcce.ac.ir/article_701405.html).
- [45] M. Négrier, E. El Ahmar, R. Sescousse, M. Sauceau, and T. Budtova, “Upcycling of textile waste into high added value cellulose porous materials, aerogels and cryogels,” *RSC Sustain.*, vol. 1, no. 2, pp. 335–345, 2023, <https://doi.org/10.1039/d2su00084a>.
- [46] M. A. Islam, M. J. Ahmed, W. A. Khanday, M. Asif, and B. H. Hameed, “Mesoporous activated carbon prepared from NaOH activation of rattan (*Lacosperma secundiflorum*) hydrochar for methylene blue removal,” *Ecotoxicol. Environ. Saf.*, vol. 138, no. January, pp. 279–285, 2017, <https://doi.org/10.1016/j.ecoenv.2017.01.010>.
- [47] A. A. Hassan and K. M. M. Al-Zobai, “Chemical oxidation for oil separation from oilfield produced water under uv irradiation using titanium dioxide as a nano-photocatalyst by batch and continuous techniques,” *Int. J. Chem. Eng.*, vol. 2019, 2019, <https://doi.org/10.1155/2019/9810728>.
- [48] M. J. Ahmed, B. H. Hameed, and E. H. Hummadi, “Review on recent progress in chitosan/chitin-carbonaceous material composites for the adsorption of water pollutants,” *Carbohydr. Polym.*, vol. 247, no. July, 2020, <https://doi.org/10.1016/j.carbpol.2020.116690>.
- [49] W. Hou, C. Ling, S. Shi, and Z. Yan, “Preparation and characterization of microcrystalline cellulose from waste cotton fabrics by using phosphotungstic acid,” *Int. J. Biol. Macromol.*, vol. 123, pp. 363–368, 2019, <https://doi.org/10.1016/j.ijbiomac.2018.11.112>.
- [50] N. A. Raheem, N. S. Majeed, and Z. Al, “Phenol Adsorption from Simulated Wastewater Using Activated Spent Tea Leaves,” *Iraqi J. Chem. Pet. Eng.*, vol. 25, no. 1, pp. 95–102, 2024, <https://doi.org/10.31699/IJCPE.2024.1.9>
- [51] H. R. D. Alamery and A. A. Hassan, “Effect of intensity of light and distance for decolonization in direct red wastewater by photo fenton oxidation,” *ARNP J. Eng. Appl. Sci.*, vol. 17, no. 1819–6608, p. 9, 2022, [http://www.arnpjournals.com/jeas/volume\\_08\\_2022.htm](http://www.arnpjournals.com/jeas/volume_08_2022.htm).
- [52] A. A. Hassan and H. T. Naeem, “Degradation of oily waste water in aqueous phase using solar (ZnO, TiO<sub>2</sub> and Al<sub>2</sub>O<sub>3</sub>) catalysts,” *Pak. J. Biotechnol.*, vol. 15, no. December, pp. 927–934, 2018, <https://pjb.org/index.php/pjbt/article/view/444>.
- [53] I. Ulhaq, W. Ahmad, I. Ahmad, M. Yaseen, and M. Ilyas, “Journal of Water Process Engineering Engineering TiO<sub>2</sub> supported CTAB modified bentonite for treatment of refinery wastewater through simultaneous photocatalytic oxidation and adsorption,” *J. Water Process Eng.*, vol. 43, no. May, p. 102239, 2021, <https://doi.org/10.1016/j.jwpe.2021.102239>.
- [54] M. A. Abu-dalo, S. A. Al-rosan, and B. A. Albiss, “Photocatalytic Degradation of Methylene Blue Using Polymeric Membranes Based on Cellulose Acetate Impregnated with ZnO Nanostructures,” *Polymers (Basel)*, pp. 1–17, 2021, <https://doi.org/10.3390/polym13193451>.
- [55] S. Raheem, A. Al-yaqoobi, H. Znad, and H. R. Abid, “Caffeine Extraction from Spent Coffee Grounds by Solid-liquid and Ultrasound-assisted Extraction: Kinetic and Thermodynamic Study,” *Iraqi J. Chem. Pet. Eng.*, vol. 25, no. 1, pp. 49–57, 2024, <https://doi.org/10.31699/IJCPE.2024.1.5>.